

If you wish to distribute this article to others, you can order high-quality copies for your colleagues, clients, or customers by [clicking here](#).

Permission to republish or repurpose articles or portions of articles can be obtained by following the guidelines [here](#).

The following resources related to this article are available online at www.sciencemag.org (this information is current as of September 24, 2010):

Updated information and services, including high-resolution figures, can be found in the online version of this article at:

<http://www.sciencemag.org/cgi/content/full/318/5849/435>

Supporting Online Material can be found at:

<http://www.sciencemag.org/cgi/content/full/1143791/DC1>

A list of selected additional articles on the Science Web sites **related to this article** can be found at:

<http://www.sciencemag.org/cgi/content/full/318/5849/435#related-content>

This article **cites 35 articles**, 2 of which can be accessed for free:

<http://www.sciencemag.org/cgi/content/full/318/5849/435#otherarticles>

This article has been **cited by** 25 article(s) on the ISI Web of Science.

This article has been **cited by** 2 articles hosted by HighWire Press; see:

<http://www.sciencemag.org/cgi/content/full/318/5849/435#otherarticles>

This article appears in the following **subject collections**:

Oceanography

<http://www.sciencemag.org/cgi/collection/oceans>

isotopic compositions varied among planetary materials. For $^{20}\text{Ne}/^{22}\text{Ne}$, the 38% difference may reflect isotopic fractionation accompanying an early loss of the terrestrial atmosphere (23), an extreme example of chemical/physical mass-dependent isotope fractionation. However, the report by Clayton in 1972 of “non-mass-dependent” O isotope fractionations (24) clearly showed that isotopic variations in volatile elements reflect isotopic inhomogeneities in the solar nebula, an unequivocal failure of the standard model.

A major problem that remains is that of understanding the differences between solar-wind isotopic noble-gas abundances and those of meteoritic (Q) noble gases (22) (Table 1). These abundances should have been similar if, as expected, Q noble gases are samples of the solar nebula trapped in meteoritic material. Can a single mass-dependent fractionation process simultaneously explain large differences in $^{20}\text{Ne}/^{22}\text{Ne}$ and small but significant differences in other noble-gas isotope ratios, such as $^{36}\text{Ar}/^{38}\text{Ar}$ between Q and solar-wind noble gases? Although fractionation during adsorption onto grain surfaces has often been discussed, the fractionation process is basically unknown.

Unlike those of Ne, Ar isotopic variations, although widely believed to exist, were not quantitatively well-defined. Isotopic ratios from spacecraft instruments such as the International Solar and Heliospheric Observatory (SOHO)/mass time-of-flight spectrometer (25) (Fig. 1) have insufficient precision to address planetary science issues (e.g., differences between solar-wind and terrestrial $^{36}\text{Ar}/^{38}\text{Ar}$ ratios). The short Apollo SWC exposure did not yield a sufficiently precise $^{36}\text{Ar}/^{38}\text{Ar}$ value to distinguish the solar and atmospheric ratios (7). A higher-than-terrestrial solar $^{36}\text{Ar}/^{38}\text{Ar}$ ratio is safely inferred from studies of lunar soils, but there has been debate on how much higher it can be, with $^{36}\text{Ar}/^{38}\text{Ar}$ values reported between 5.48 and 5.80 (26, 27). Corrections for excess ^{38}Ar from galactic-cosmic-ray nuclear reactions present a challenge in interpreting lunar-soil data. Genesis data require negligible galactic-cosmic-ray corrections. This, plus higher analytical precision, significantly improves the accuracy of the solar-wind and the atmospheric $^{36}\text{Ar}/^{38}\text{Ar}$ difference. Our solar-wind $^{36}\text{Ar}/^{38}\text{Ar}$ ratio (Table 1) is higher than that of the terrestrial atmosphere by $3.42 \pm 0.09\%$. This should lead to improved constraints on models for terrestrial atmospheric loss. It is also significantly higher than the $^{36}\text{Ar}/^{38}\text{Ar}$ value of “Q”.

The significantly increased precision of Ne and Ar solar-wind isotopic compositions have yielded no differences among the Genesis regime samples. Nevertheless, we have not proved that there is no Ne or Ar isotopic fractionation between the Sun and the solar wind. Our data clearly put a constraint on such fractionations, but at present the strength of the constraint is not known. A “unified” theoretical approach evaluating FIP and coulomb drag fractionations in the context of formation models of the different solar-wind regimes is required. If fractionations between the Sun and the solar wind are large but the same for

all regimes, then the absence of inter-regime isotopic variations is inconclusive. Alternatively, the fractionations among regimes could be large and the lack of inter-regime variations quite constraining. The goal of the Genesis mission is to provide higher-precision solar-wind composition data, leading to better theories of solar-wind fractionations, which, in turn, will lead to improved solar abundances for planetary science purposes.

References and Notes

- H. Palme, A. Jones, in vol. 1 of *Treatise of Geochemistry*, A. M. Davis, Ed. (Elsevier, Amsterdam, 2003), chap. 3, pp. 41–61.
- R. N. Clayton, in vol. 1 of *Treatise of Geochemistry*, A. M. Davis, Ed. (Elsevier, Amsterdam, 2003), chap. 6., pp. 129–142.
- H. Busemann *et al.*, *Science* **312**, 727 (2006).
- R. Wieler, H. Busemann, I. Franchi, in *Meteorites and the Early Solar System II*, D. S. Lauretta, H. McSween Jr., Eds. (Univ. of Arizona, Tucson, AZ, 2006), part vi, pp. 499–521.
- Nuclear-energy generation in the interior of the Sun has produced significant elemental and isotopic changes, but matter is not exchanged between the inner and outer regions, so with a few exceptions, the composition of the solar surface has remained unchanged since the beginning of the solar system.
- J. Geiss, G. Gloeckler, *Space Sci. Rev.* **106**, 3 (2003).
- J. Geiss *et al.*, *Space Sci. Rev.* **110**, 307 (2004).
- R. von Steiger *et al.*, *Space Sci. Rev.* **97**, 123 (2001).
- R. von Steiger, J. Geiss, *Astron. Astrophys.* **225**, 222 (1989).
- J. Geiss, P. Hirt, H. Leutwyler, *Solar Phys.* **12**, 458 (1970).
- R. Bodmer, P. Bochsler, *Astron. Astrophys.* **337**, 921 (1998).
- D. S. Burnett *et al.*, *Space Sci. Rev.* **105**, 509 (2003).
- M. Neugebauer *et al.*, *Space Sci. Rev.* **105**, 661 (2003).
- D. B. Reisenfeld *et al.*, *Am. Inst. Phys. Conf. Proc.* **679**, 632 (2003).
- J. C. Mabry *et al.*, *Lunar Planet. Sci. Conf. XXXVIII*, abstr. 1338 (2007).
- Materials and methods are available as supporting material on Science Online.
- C. M. Hohenberg, N. Thonnard, A. Meshik, *Meteorit. Planet. Sci.* **37**, 257 (2002).
- V. S. Heber, H. Baur, D. Burnett, R. Wieler, *Lunar Planet. Sci. Conf. XXXVIII*, abstr. 1894 (2007).
- A. Grimberg *et al.*, *Science* **314**, 1133 (2006).
- S. Basu, H. M. Antia, *Astrophys. J.* **606**, L85 (2004).
- J. Geiss, G. Gloeckler, R. von Steiger, *Space Sci. Rev.* **72**, 49 (1995).
- M. Ozima, R. Wieler, B. Marty, F. Podosek, *Geochim. Cosmochim. Acta* **62**, 301 (1998).
- R. O. Pepin, *Earth Planet. Sci. Lett.* **252**, 1 (2006).
- R. N. Clayton, *Earth Planet. Sci. Lett.* **13**, 455 (1972).
- J. M. Weygand, F. Ipavich, P. Wurz, J. Paquette, P. Bochsler, *Geochim. Cosmochim. Acta* **65**, 4589 (2001).
- J.-P. Benkert, H. Baur, P. Signer, R. Wieler, *J. Geophys. Res. (Planets)* **98**, 13147 (1993).
- R. L. Palma, R. Becker, R. Pepin, D. Schlutter, *Geochim. Cosmochim. Acta* **66**, 2929 (2002).
- H. Cerutti, thesis, Univ. of Bern (1974).
- A. O. Nier, *Phys. Rev.* **77**, 789 (1950).
- We acknowledge the support of the entire Genesis team in enabling this work. Portions of this work at Washington Univ. were supported by NASA grants (NNJ04H117G and NAG5-12885).

Supporting Online Material

www.sciencemag.org/cgi/content/full/318/5849/433/DC1
SOM Text
Fig. S1
Tables S1 and S2
References
22 May 2007; accepted 31 August 2007
10.1126/science.1145528

Southern Hemisphere and Deep-Sea Warming Led Deglacial Atmospheric CO₂ Rise and Tropical Warming

Lowell Stott,^{1*} Axel Timmermann,² Robert Thunell³

Establishing what caused Earth’s largest climatic changes in the past requires a precise knowledge of both the forcing and the regional responses. We determined the chronology of high- and low-latitude climate change at the last glacial termination by radiocarbon dating benthic and planktonic foraminiferal stable isotope and magnesium/calcium records from a marine core collected in the western tropical Pacific. Deep-sea temperatures warmed by ~2°C between 19 and 17 thousand years before the present (ky B.P.), leading the rise in atmospheric CO₂ and tropical-surface-ocean warming by ~1000 years. The cause of this deglacial deep-water warming does not lie within the tropics, nor can its early onset between 19 and 17 ky B.P. be attributed to CO₂ forcing. Increasing austral-spring insolation combined with sea-ice albedo feedbacks appear to be the key factors responsible for this warming.

The data obtained from high-latitude ice cores establish a close temporal relation between varying concentrations of atmospheric CO₂ and atmospheric temperatures during glacial terminations (1). However, uncertainty in the gas-age chronologies and inadequate temporal resolution in many proxy climate reconstructions have hampered efforts to establish the

exact phasing of events during glacial terminations, a necessary step in understanding the physical relation between CO₂ forcing and climate change (2). Arguably, the most robust estimate of changes in mean global temperatures that accompany glacial terminations is the amount of heat stored in the oceans. The large size of the oceanic reservoir and the long residence time of

deep waters mean that deep-water temperatures reflect a globally averaged record of Earth's radiative-heat balance (3). At present, we cannot quantify changes in ocean heat content at the last glacial termination. However, because deep waters formed at high latitudes carry with them the nearly conservative properties of temperature and salinity, it is possible to establish the relative timing of high-latitude versus low-latitude climatic change at glacial terminations by dating co-occurring benthic (bottom-dwelling) and planktonic (surface-dwelling) foraminiferal paleotemperature records in a marine core from a tropical location that has sufficient temporal resolution. We used radiocarbon (^{14}C) dating to establish the timing of the deep-sea and tropical-surface-ocean temperature changes during the last glacial termination and compared this history with the timing of CO_2 change and deglacial warming in the southern high latitudes during the last glacial termination.

Marine sediment core MD98-2181 from the Morotai Basin (Fig. 1) is ideally suited for documenting the timing of both deep-sea and tropical-surface-water temperature change during the last glacial termination because the sediments at this site are an admixture of planktonic and benthic foraminiferal carbonate that accumulated at rates of 50 to 80 cm/thousand years (ky) over the past glacial-to-interglacial transition (4). Sampling this core at the centimeter scale provides a temporal resolution for each sample of ~25 to 50 years (5). This core was recovered from a depth of 2114 m, where it was bathed in the upper Pacific Deep Water, a water mass whose temperature and salinity are acquired within the Southern Ocean (6). The site is also located within the Pacific Warm Pool (7), where the $\delta^{18}\text{O}$ and Mg/Ca of planktonic foraminifera record the temperature and salinity of western tropical Pacific surface water (8, 9).

We compiled 42 planktonic (4) and 8 mixed-benthic (Table 1) ^{14}C ages from late glacial and Holocene sections of this site (Fig. 2). Broecker *et al.* (10) noted previously that the benthic/planktonic ^{14}C age difference from the glacial termination horizons of this core averages ~1300 years, similar to the ^{14}C offset between surface and deep waters today (fig. S2). Of the eight benthic/planktonic pairs we have from the deglacial section, the average age difference is 1493 (± 367) years, similar to Broecker *et al.*'s estimate. The reservoir age of surface waters in the source region of the Pacific Deep Water may have been slightly older during the glacial period, which would explain the somewhat higher surface/deep-water age difference in the glacial samples (11). However, given the small range in $\Delta^{14}\text{C}$, we

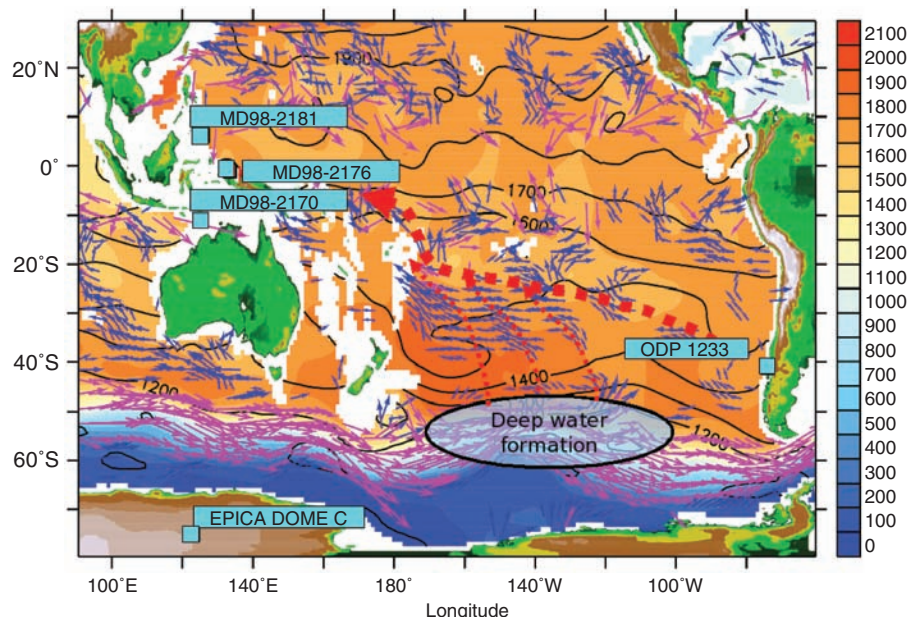
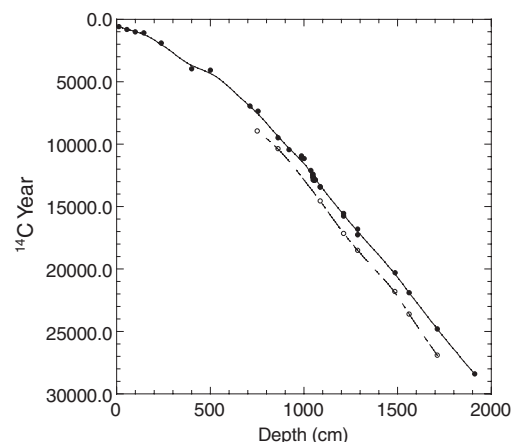


Fig. 1. Location of tropical sites (MD98-2181, MD98-2176 and MD98-2170), high-southern latitude Ocean Drilling Program site 1233, and the EPICA Dome C ice core. At 2100 m, the MD98-2181 site is bathed by the Pacific Deep Water (supporting online material). The depth of the isopycnal surface $\sigma_t = 27.6 \text{ kg/m}^3$ (relative to the 0 m) is shown with color shading (39), pre-bomb ^{14}C ages from the Global Data Analysis Project data set (40) are interpolated onto $\sigma_t = 27.6 \text{ kg/m}^3$ (contour lines), geostrophic velocity on $\sigma_t = 27.6 \text{ kg/m}^3$ is shown (blue and magenta vectors, the scale of the magenta vectors is reduced by 60% relative to the blue vectors for better visibility), and the locations of marine cores are indicated.

Table 1. Benthic foraminiferal ^{14}C ages from the Morotai Basin core MD98-2181 (6°N, 126°E, 2.1 km). All ^{14}C measurements were conducted at the Woods Hole Accelerator Laboratory. NOSAMS, National Ocean Sciences Accelerator Mass Spectrometry.

Depth (cm)	NOSAMS accession number	Benthic species	^{14}C age (years)	Error (years)
751	OS-55868	<i>C. mundula</i>	8,950	50
861	OS-55869	<i>C. mundula</i>	10,350	65
1086	OS-54924	<i>C. mundula</i>	14,550	70
1211	OS-54928	Mixed benthics	17,150	85
1286	OS-54925	Mixed benthics	18,500	130
1486	OS-55820	Mixed benthics	21,800	95
1561	OS-60238	Mixed benthics	23,600	160
1711	OS-60246	Mixed benthics	26,900	120

Fig. 2. ^{14}C ages of planktonic (solid circles) and benthic foraminifers (open circles) from MD98-2181. The average benthic/planktonic ^{14}C age difference is 1493 (± 367) years through the late glacial and early deglacial portion of the core. ^{14}C dates for terrestrial wood from the glacial section indicates that the surface reservoir age in the Western tropical Pacific was not much higher during the glacial period (10). ^{14}C data from 941 to 961 cm were excluded because of a sediment disturbance at this depth (4).



¹Department of Earth Sciences, University of Southern California, Los Angeles, CA 90089, USA. ²International Pacific Research Center (IPRC), School of Ocean and Earth Science and Technology, University of Hawaii, Honolulu, HI 96822, USA. ³Department of Geological Sciences, University of South Carolina, Columbia, SC 29208, USA.

*To whom correspondence should be addressed. E-mail: stott@usc.edu

see no evidence for a substantial shift in the surface/deep-water age difference and therefore estimate that the transit time of deep water from the Southern Ocean to the north equatorial Pacific was ~ 1000 (± 300) years during the glacial

period, as in the modern ocean (12). The conversion of ^{14}C ages to a calendar-age model was performed with the CALIB 5.0.2 routine using the Marine04 calibration data set (13). A reservoir-age correction of 560 years was applied for the plank-

tonic samples younger than 13,000 years; a correction of 630 years was applied for older samples. At each stratigraphic horizon, the benthic foraminiferal $\delta^{18}\text{O}$ value reflects the deep-water temperature and oxygen isotope composition acquired from the Southern Ocean ~ 1000 years earlier (fig. S2). Therefore to compare the temporal phasing of deep-water- and tropical-surface-water changes at the deglaciation, an independent chronology was established for the benthic $\delta^{18}\text{O}$ record by adding 1000 years to the planktonic calendar age at each core horizon.

Previous studies (8, 9, 14–18) have shown that during the last glacial termination, tropical Pacific sea surface temperatures (SSTs) began to warm at ~ 17.5 thousand years before the present (ky B.P.) and that the warming preceded the first major shift in seawater $\delta^{18}\text{O}$ associated with the disintegrating glacial ice sheets (17). The timing of tropical SST warming is best documented in the MD98-2181 core, which has the highest sediment-accumulation rate and the most detailed ^{14}C age control of the available cores (fig. S1). However, two other closely associated cores, MD98-2176 and MD98-2170, compliment the MD98-2181 SST record and provide a composite representation of the Western Pacific Warm Pool during the last deglaciation (8). During the Last Glacial Maximum, the SSTs at these sites averaged 26°C (Fig. 3) (8, 9). SSTs increased by $\sim 1^\circ\text{C}$ between 17 and 16 ky B.P., and by 14.6 ky B.P. they had reached $\sim 28^\circ\text{C}$ across the Warm Pool. The deglacial warming within the tropical Pacific Warm Pool occurred in close association with increasing concentrations of atmospheric CO_2 (14); this finding has provided support for hypotheses that call on the CO_2 increase itself to explain the deglacial warming (19–21). However, the exact phasing between the CO_2 increase and the tropical SST warming is not well established because of the uncertainty in assigning gas ages to CO_2 records (1, 22–24). In the Dome C ice core, for example, the concentrations of both CO_2 and CH_4 begin to increase above their glacial values at 525 m. In the European Project for Ice Coring in Antarctica (EPICA) Dome C 2 (I) time scale, this corresponds to a gas age of 17.3 ky B.P., which would mean that the initial rise in CO_2 occurred essentially simultaneously with warming in the tropical Pacific. However, by synchronizing CH_4 records from the Antarctic Dome C core and the Greenland Ice Sheet Project (GISP) core (23) and adopting the GISPII gas-age model, the initial CO_2 rise could be shifted to as early as 18 ky B.P. and therefore slightly earlier than the tropical SST warming (Fig. 3). In either case, the concentration of atmospheric CO_2 did not begin to rise until after 19 ky B.P.

If atmospheric CO_2 was the sole driver of deglacial temperature changes, the deep-sea temperatures should reflect this with an appropriate lagged relation that would account for the response time between CO_2 forcing and the turnover time of deep waters. The Pacific is the best candidate for testing the temporal relation because

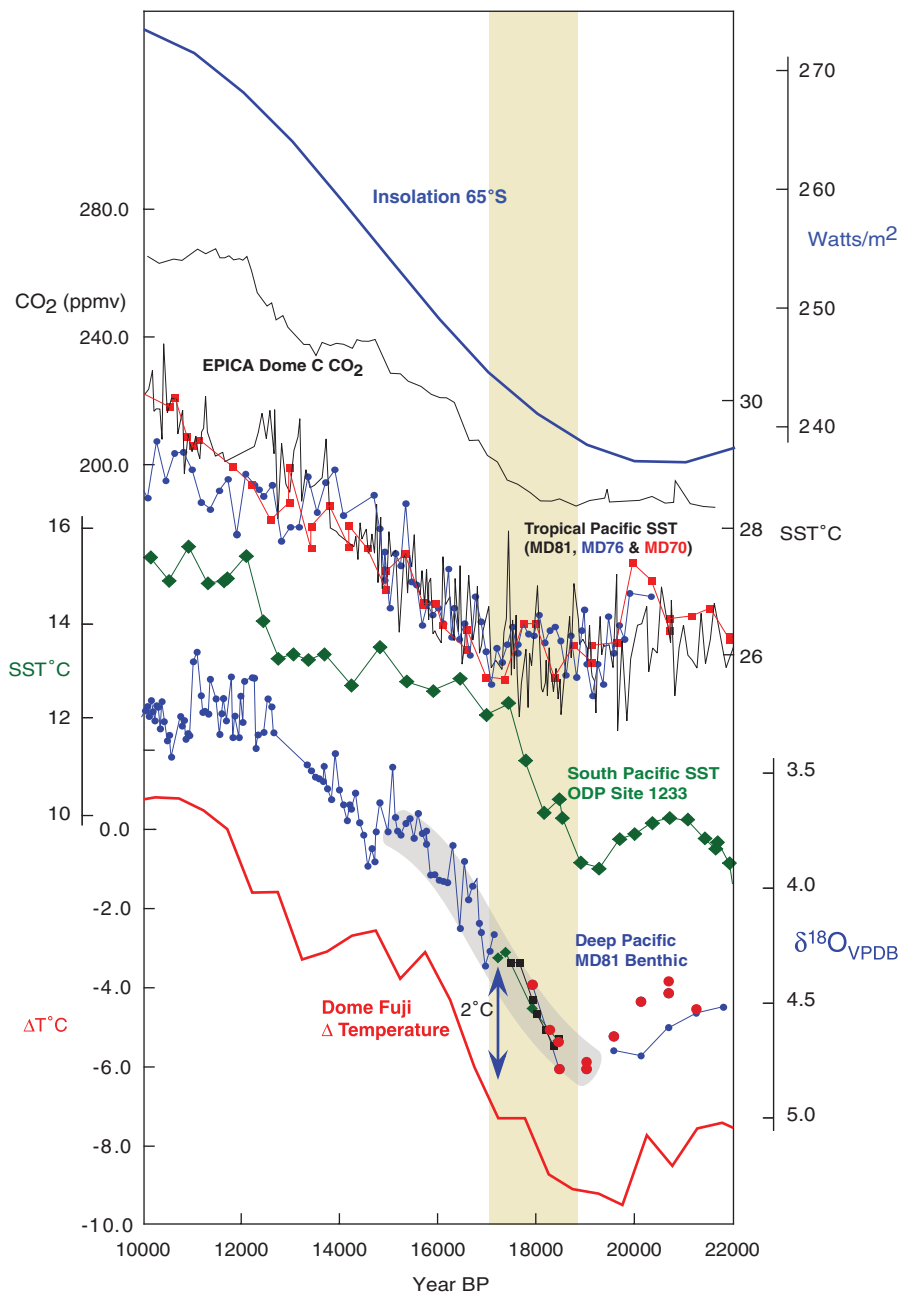


Fig. 3. Temporal phasing of the Pacific deep- and tropical-surface-water deglacial stratigraphy compared with the EPICA Dome C CO_2 record (1). The averaged mean longitude spring insolation (21 August to 20 November) at 65°S insolation and the Dome Fuji ice core temperature deviation (ΔT_{site}) relative to the mean of the last 10 thousand years is shown (34). The yellow shading spans the time period between the initial warming of deep-sea temperatures and the onset of tropical Pacific SST warming. The Dome C CO_2 record was plotted on the GISPII gas-age model (15) by synchronizing the GISP II and Dome C CH_4 stratigraphies. The deep Pacific $\delta^{18}\text{O}$ record is based on multiple species of benthic foraminifera from MD98-2181 (*Cibicides mundula*, blue circles; *Uvigerina costata*, red circles; *Uvigerina hispida*, black squares; *Cibicides wuellerstorffii*, green diamonds; red squares, *Uvigerina* sp.) and is depicted on an age scale that represents the surface conditions at the source region of the Pacific Deep Water. The gray shading indicates a ~ 200 -year uncertainty in the benthic ages. A disturbed interval between the 941- and 961-cm sections of MD98-2181 encompassing the interval associated with the Antarctic Cold Reversal is excluded. ppmv, parts per million by volume; VPDB, Vienna Pee Dee belemnite.

it is volumetrically the largest deep-water reservoir. Shackleton (19) recognized the phasing similarity between $\delta^{18}\text{O}$ of O_2 gas trapped in the Vostok ice core (25) and the orbital-insolation record (June insolation at 65°N) and argued that the O_2 record reflects the influence of solar-insolation forcing vis-à-vis ice-volume variations. He tuned the deep-sea (benthic) $\delta^{18}\text{O}$ record from Pacific core VM19-30 to the Vostok O_2 $\delta^{18}\text{O}$ stratigraphy and applied the orbital-insolation chronology to it. The advantage of this approach would be to provide an estimate of the deep-sea temperature change, which is the residual benthic $\delta^{18}\text{O}$ signal that is not accounted for by the Vostok O_2 $\delta^{18}\text{O}$ record. However, this method also imposed a phase relation between the deep-sea temperature change and the ice-volume components of the benthic $\delta^{18}\text{O}$ record. As a result, the "tuned" VM19-30 benthic $\delta^{18}\text{O}$ record does not exhibit any deglacial $\delta^{18}\text{O}$ change until ~ 15 ky B.P., nearly 3000 years after atmospheric CO_2 began to rise (fig. S2). In a subsequent study of deep Pacific temperature changes during the last glacial termination, Martin *et al.* (20) used Mg/Ca-based estimates of benthic temperature change to argue that deep Pacific temperatures warmed by 2°C during the glacial termination and that the magnitude of these deep-sea temperature changes was consistent with a forcing by CO_2 during the deglaciation. Here again, the issue is timing. Did deep-sea temperature change lag the CO_2 forcing? The records used by Martin *et al.* (20) to argue for the CO_2 forcing of deep-sea temperatures were also tuned to the orbital-insolation record through a cross correlation of benthic $\delta^{18}\text{O}$ records to Shackleton's VM19-30 record. Consequently, these cores do not provide an independent constraint on the temporal relation between temperature change and CO_2 concentration.

We circumvented the assumptions associated with tuning benthic records by independently dating benthic foraminifera from MD98-2181 (Table 1). In Fig. 3, the independently dated MD98-2181 benthic $\delta^{18}\text{O}$ stratigraphy (representing Southern Ocean surface conditions 1000 years earlier) is compared with the western tropical Pacific SST reconstructions. The maximum benthic $\delta^{18}\text{O}$ values occurred between 20 and 19 ky B.P. Three species of benthic foraminifera exhibited a $\delta^{18}\text{O}$ value of 4.8 per mil (‰) during this time period, a value that is 1.8‰ higher than modern benthic values at this site. Taking the mean ocean glacial-to-interglacial $\delta^{18}\text{O}$ shift to be 1‰ (19, 26–30), the observed 1.8‰ difference between Holocene and glacial $\delta^{18}\text{O}$ values at MD98-2181 implies that temperatures at 2100 m in the Pacific were $\sim 2.5^\circ\text{C}$ colder and/or the $^{18}\text{O}/^{16}\text{O}$ of the deep water was substantially higher at the glacial maximum. Pore-water Cl profiles from deep-sea sediment cores suggest that deep waters were more salty during the Last Glacial Maximum, perhaps by as much 1‰ (30), but there is no evidence to suggest that the $^{18}\text{O}/^{16}\text{O}$ of the Pacific deep water was substantially higher (after correcting for the 1‰ ice-volume

effect) (31). Considering these results together with the Mg/Ca data from the eastern Pacific (32) indicates that the primary influence on the early deglacial benthic $\delta^{18}\text{O}$ evolution was temperature change. The benthic $\delta^{18}\text{O}$ values from MD98-2181 began to decrease from the cold glacial maximum values at 19 to 18.5 ky B.P. and decreased progressively by $\sim 0.5\%$ over the next 1000 years. If this 0.5‰ decrease was entirely due to temperature, it means that nearly all of the glacial/interglacial deep-water warming occurred before 17.5 ky B.P. and therefore before both the onset of deglacial warming in tropical Pacific surface waters and the increase in atmospheric CO_2 concentration.

A comparable warming has also been observed in surface-water records from the mid-latitudes in the south Pacific (33). At this latitude the surface waters also warmed by 2°C between 19 and 17 ky B.P., leading the tropical warming by ~ 1000 years (Fig. 2). The onset and temporal evolution of deglacial warming over the Antarctic continent (34) also matches the deep-ocean record of warming (Fig. 3). These records, together with the synchronous retreat of mid-southern-latitude glaciers (35), confirm that the onset of deglacial warming throughout the Southern Hemisphere occurred long before deglacial warming began in the tropical surface ocean. An early warming in the Antarctic has important implications for understanding what may have caused an asynchronous deglacial warming pattern between the low and high southern latitudes. In particular, it means that the mechanism responsible for initiating the deglacial events does not lie directly within the tropics itself, nor can these events be explained by CO_2 forcing alone. Both CO_2 and the tropical SSTs did not begin to change until after 18 ky B.P. (22), approximately 1000 years after the benthic $\delta^{18}\text{O}$ record indicates that the Southern Ocean was warming.

The rise in Southern Ocean temperatures coincided with the retreat of Antarctic sea ice and high-elevation glaciers in the Southern Hemisphere (36, 37). The explanation for the early warming in the Southern Hemisphere could involve increasing springtime solar insolation, which is well correlated with the retreat of sea ice and with the history of sea-salt accumulation in the Antarctic Dome C ice core (fig. S5). We suggest that the trigger for the initial deglacial warming around Antarctica was the change in solar insolation over the Southern Ocean during the austral spring that influenced the retreat of the sea ice (38). Retreating sea ice would have led to enhanced Ekman transport in the Southern Ocean and decreased stratification due to stronger air-sea fluxes. We hypothesize that these forcings promoted enhanced ventilation of the deep sea and the subsequent rise in atmospheric CO_2 .

References and Notes

1. EPICA Community Members, *Nature* **429**, 623 (2004).
2. P. Köhler, H. Fischer, G. Munhoven, R. E. Zeebe, *Global Biogeochem. Cycles* **19**, GB4020 (2005).

3. T. P. Barnett, D. W. Pierce, R. Schnur, *Science* **292**, 270 (2001).
4. L. Stott, *Paleoceanography* **22**, PA1211 (2007).
5. Materials and methods are available as supporting material on Science Online. In the supporting material, we also present our ^{14}C data and age model details for cores MD98-2176 and MD98-2170 (fig. S1).
6. Details about the Pacific Deep Water formation and circulation are given in the supporting material.
7. M. Ioualalen *et al.*, *Geophys. Res. Lett.* **27**, 1243 (2000).
8. L. Stott *et al.*, *Nature* **431**, 56 (2004).
9. L. Stott, C. Poulsen, S. Lund, R. Thunell, *Science* **297**, 222 (2002).
10. W. Broecker *et al.*, *Science* **306**, 1169 (2004).
11. E. L. Sikes, C. R. Samson, T. P. Guilderson, W. R. Howard, *Nature* **405**, 555 (2000).
12. The distribution pre-bomb ^{14}C ages within the Pacific are illustrated in fig. S3. The ^{14}C age of the Pacific Deep Water increases by ~ 1000 years between the Southern Ocean and the tropical Pacific.
13. K. A. Hughen *et al.*, *Radiocarbon* **46**, 1059 (2004).
14. D. W. Lea, D. K. Pak, H. J. Spero, *Science* **289**, 1719 (2000).
15. M. K. Gagan, E. J. Hendy, S. G. Haberler, W. S. Hantoro, *Quat. Int.* **118–119**, 127 (2004).
16. D. W. Oppo, B. K. Linsley, Y. Rosenthal, S. Dannenmann, L. Beaufort, *Geochim. Geophys. Geosyst.* **4**, 1003 (2003).
17. K. Visser, R. Thunell, L. Stott, *Nature* **421**, 152 (2003).
18. T. Kiefer, M. Kienast, *Quat. Sci. Rev.* **24**, 1063 (2005).
19. N. J. Shackleton, *Science* **289**, 1897 (2000).
20. P. Martin, D. Archer, D. W. Lea, *Paleoceanography* **20**, PA2015 (2005).
21. D. W. Lea, *J. Clim.* **17**, 2170 (2004).
22. E. Monnin *et al.*, *Science* **291**, 112 (2001).
23. T. Blunier, E. J. Brook, *Science* **291**, 109 (2001).
24. L. Loulergue *et al.*, *Clim. Past Discuss.* **3**, 435 (2007).
25. J. R. Petit *et al.*, *Nature* **399**, 429 (1999).
26. J. F. Adkins, D. P. Schrag, *Geophys. Res. Lett.* **28**, 771 (2001).
27. K. Lambeck, J. Chappell, *Science* **292**, 679 (2001).
28. D. P. Schrag, G. Hampt, D. W. Murray, *Science* **272**, 1930 (1996).
29. J. Chappell, *Quat. Sci. Rev.* **21**, 1229 (2002).
30. J. F. Adkins, K. McIntyre, D. P. Schrag, *Science* **298**, 1769 (2002).
31. D. P. Schrag *et al.*, *Quat. Sci. Rev.* **21**, 331 (2002).
32. P. A. Martin *et al.*, *Earth Planet. Sci. Lett.* **198**, 193 (2002).
33. J. Kaiser, F. Lamy, D. Hebbeln, *Paleoceanography* **20**, PA4009 (2005).
34. K. Kawamura *et al.*, *Nature* **448**, 912 (2007).
35. J. M. Schaefer *et al.*, *Science* **312**, 1510 (2006).
36. A. Shemesh *et al.*, *Paleoceanography* **17**, 1056 (2002).
37. T. T. Barrows, J. O. Stone, L. K. Fifield, *Quat. Sci. Rev.* **23**, 697 (2004).
38. The sea-salt Na accumulation in Antarctic ice cores (fig. S5) is interpreted here as a proxy for sea-ice coverage around Antarctica.
39. S. Levitus, *Climatological Atlas of the World Ocean* (U.S. Government Printing Office, Washington, DC, 1994).
40. R. M. Key *et al.*, *Global Biogeochem. Cycles* **18**, GB4031 (2004).
41. L.S., R.T., and A.T. were supported by grants from the Marine Geology and Geophysics and the Atmospheric Sciences Paleoclimatology Programs of NSF. A.T. is supported by the Japan Agency for Marine-Earth Science and Technology through its sponsorship of the International Pacific Research Center. This is IPRC Publication number 471. We thank M. Rincon for analytical support and O. Timm for many stimulating discussions.

Supporting Online Material

www.sciencemag.org/cgi/content/full/1143791/DC1

Materials and Methods

SOM Text

Figs. S1 to S5

Table S1

References

13 April 2007; accepted 11 September 2007

Published online 27 September 2007;

10.1126/science.1143791

Include this information when citing this paper.